Molecular Iodine for a General Synthesis of Binary and Ternary Inorganic and Hybrid Organic-inorganic Iodide Nanocrystals

Quinten A. Akkerman,[†,‡] Laura Martínez-Sarti[⊥], Luca Goldoni,[//] Muhammad Imran,[†,‡] Dmitry Baranov,[†] Henk J. Bolink[⊥], Francisco Palazon*[⊥] and Liberato Manna*[,†]

[†]Department of Nanochemistry, [//]Analytical Chemistry Facility, Istituto Italiano di Tecnologia, Via Morego 30, 16163 Genova, Italy

[‡]Dipartimento di Chimica e Chimica Industriale, Università degli Studi di Genova, Via Dodecaneso 31, 16146 Genova, Italy

[⊥]Instituto de Ciencia Molecular, Universidad de Valencia, C/ Catedrático J. Beltrán 2, 46980 Paterna, Spain

KEYWORDS. Nanocrystals, metal iodides, perovskites, LEDs

ABSTRACT: We report the synthesis of various binary and ternary inorganic and hybrid organic-inorganic iodide nanocrystals starting from molecular iodine (I_2). The procedure utilizes a reaction between I_2 and oleylamine that yields oleylammonium iodide – the iodide precursor for a subsequent preparation of nanocrystals. The syntheses are facile, carried out under air, in vials heated on a hotplate and deliver nanocrystals with narrow size distributions and, in the case of red and near infrared-emitting lead-based perovskites, with 70-80% photoluminescence quantum yields. The The latter were used to fabricate red and infrared bright light-emitting diodes, with external quantum efficiencies (EQE) exceeding 3%.

Metal halide nanocrystals (NCs) have gained increasing attention in past years.[1-3] Among these metal halide NCs, the halide perovskite ($APbX_3$ with A = Cs^+, methyl ammonium (MA) or formamidinium (FA), B = Pb^{2+} or Sn^{2+} and X = Cl^-, Br^- or I^-) NCs are by far the most studied ones, due to their excellent optical properties and their relatively simple synthesis methods.[1-2, 4] The strong interest in these halide perovskite NCs has also motivated the development of synthesis approaches for other colloidal halide based NCs. This interest is mainly driven by the search for lead-free perovskite alternatives to the Pb-based ones for applications in photovoltaics and lighting. This has led for instance to reports on synthesis of ternary Cs_2SnI_6, $Cs_3Bi_2X_9$ and $Cs_3Sb_2X_9$ NCs, and quaternary Cs_2AgBiX_6 double perovskite NCs.[5-9] Another group of interesting new metal halide NCs emerging from the perovskite NC research are the Cs_4PbX_6 NCs, as well as simple cesium halide NCs.[10-11]

The vast majority of colloidal metal halide NCs are nowadays prepared based on the colloidal synthesis scheme of $CsPbX_3$ NCs reported by Protesescu *et al.*,[1] were a Cs-oleate solution is quickly injected into a hot solution of the metal halide precursor (for example PbX_2) dissolved in octadecene (ODE), oleylamine (OLAM) and oleic acid (OA). Although this method yields high quality perovskite NCs, it does not allow to control the Pb:halide molar ratio introduced in the synthesis and moreover it relies strongly on the solubility of the metal halide precursors in the ligand/solvent mixture. Also, this method cannot be generalized, as many metal halides (for example AgBr and $PbCl_2$) are difficult to dissolve in simple OA and OLAM mixtures and additional ligands (like trioctyl phosphine oxide) are required. Other issues are related to the high costs and instability of certain metal halide salts, like for example most transition metal iodides.[1, 12] These precursors are often highly reactive, and not much work has been done towards controlling the precursor reactivity, as opposed to the extensive research devoted to identify suitable chemicals for the synthesis of the more traditional cadmium and lead chalcogenide NCs.[13-14] Developing synthetic methods where elemental ratios, especially between cations and anions, can be tuned independently, is an important goal in the preparation of multinary materials, and is also relevant for metal halide perovskites. To this end, both Creutz *et al.* and Imran *et al.* recently reported a different method to prepare metal halide NCs, where a reactive halide precursor (either trimethylsilyl halide or benzoyl halide) is injected into a solution of metal acetate salts.[15-16] Imran *et al.* for example demonstrated that this synthesis can be extended to various perovskite $APbX_3$ NCs by simply choosing the proper precursors and optimizing the reaction conditions.[16] Although the use of trimethylsilyl halides or benzoyl halides resulted in perovskite and double perovskite NCs with narrow size distributions, these chemicals are air sensitive, which prevents their use in the syntheses under ambient conditions (i.e. under air).

Here, we report a general synthesis route to binary and ternary inorganic and hybrid organic-inorganic iodide NCs based on the injection of an OLAM-I_2 solution in an ODE solution containing metal or organic oleates. By selecting the appropriate metal or organic salt precursor, and by optimizing the OA concentration and reaction temperature, inorganic and hybrid organic-inorganic iodide NCs of various compositions were prepared. All syntheses were performed under air, on a hotplate with off-the-shelf chemicals, highlighting the ease of the process and potential for high throughput synthesis. The nearly monodisperse lead iodide perovskite NCs prepared by this method had photoluminescence quantum yields (PLQYs) close to 80% and good stability over at least several weeks

in air. These NCs were implemented as active layers in red and infrared light-emitting diodes with external quantum efficiencies (EQE) exceeding 3%. Additionally, other NCs such as $Cs_3Bi_2I_9$ and CsI NCs, and also several materials which have not yet been reported in the form of colloidal NCs, such as AgI, RbI, KI, $FA_3Bi_2I_9$ and $RbAg_4I_5$ could be synthesized.

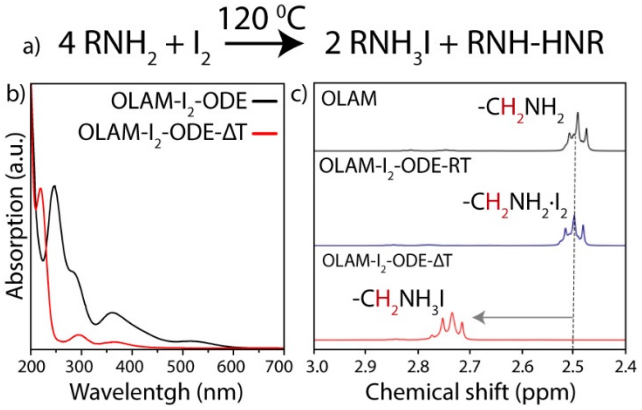

Figure 1. Formation of the oleylammonium precursor. a) Proposed reaction of iodine and oleylamine, leading to oleylammonium iodine (see also reaction scheme SI1); b) Optical absorption spectra of the OLAM-I_2 mixture before and after heating to 120 ^{0}C, indicting the appearance of I^- species after heating (absorption band at around 220 nm); c) Selected region of ^{1}H NMR spectra of the OLAM-I_2 before and after heating to 120 ^{0}C. Upon heating, OLAM is protonated. Full spectra and assignment of resonances are reported in Figure SI2.

The iodide precursor used in the synthesis of the various NCs reported here was prepared by heating solid grains of molecular I_2 in a solution of ODE and OLAM. This led to the *in situ* formation of oleylammonium iodide (Figure 1a). Such oleylammonium iodide/oleylamine precursor solution remained stable and no precipitate was seen at room temperature, even when stored in air. The same type of solution has been previously used by us to convert $CsPbBr_3$ to $CsPbI_3$ by anion-exchange.[17] The mechanism leading to alkyl ammonium iodide by reacting amines with iodine has been already hypothesized in the 70s:[18] it was proposed that the reaction goes through an oleylamine-iodide charge transfer complex, followed by a proton-iodine exchange, resulting in alkyliodoamine, hydro iodic acid and triiodide species (Scheme SI1 of the Supporting Information, SI,).[18] Finally, the *in situ* formed HI reacts with the alkylamine, resulting in the alkylammonium iodide. This last step coincides with the synthesis of alkylammonium halides by reaction of amines with hydrogen halide solutions.[4] Although it is difficult to confirm the formation of the various intermediates (and actually beyond the scope of this work), the presence of oleylammoniuim iodide can be proved with both optical absorption and nuclear magnetic resonance (NMR) spectroscopy. When, in our experiments, I_2 was dissolved in OLAM at room temperature, the solution turned quickly dark brown and featured three absorption bands peaked at 520 nm, 360 nm, and 280 nm, which are ascribed to the I_2 charge transfer complexes and to HI_3 (Figure 1b).[18-20] When the solution was heated up 120 ^{0}C, it quickly turned light brown (Figure SI1). The appearance of I^- (hence of oleylammonium iodide) upon heating could be tracked by optical absorption spectroscopy, as shown in Figure 1b. Here, the lower energy absorptions bands disappeared and a new strong absorption appeared at around 220 nm, matching that of previous reports on I^-.[19, 21] ^{1}H NMR spectra of the OLAM-I_2 mixture were recorded before and after heating, as reported in Figure 1c and SI2. Before heating, resonances of the CH_2 in position α to the nitrogen of OLAM remained unchanged, indicating that under these conditions the amine does not get protonated, but it is rather engaged in a charge transfer complex with I_2.[19] After the OLAM-I_2 solution was heated to 120 ^{0}C, the α-CH_2 peaks exhibited an increase in chemical shift of 0.22 ppm. The extent of the chemical shift is close to that of the α-CH_2 peaks of OLAM in a 1: 1 mixture with oleic acid, as discussed in a previous work of us, and ascribed to the protonation of OLAM.[22]

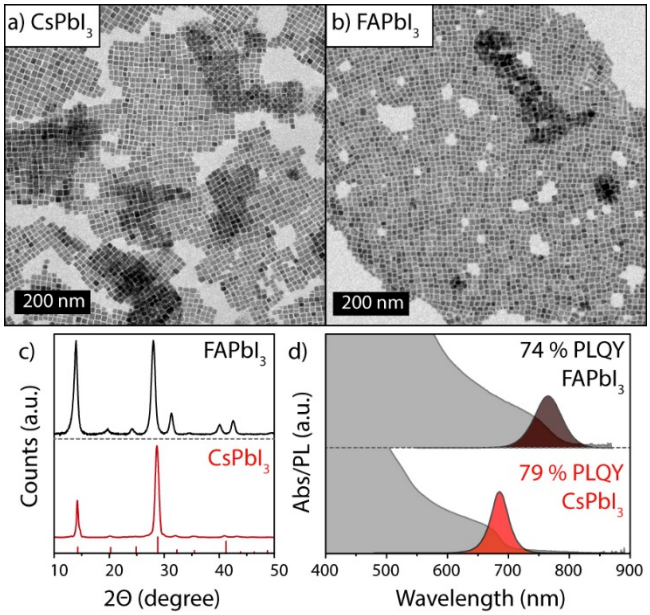

Figure 2. Lead iodide perovskite NCs. a-b) TEM images of $CsPbI_3$ and $FAPbI_3$ NCs indicating narrow size distributions; c) XRD pattern of $CsPbI_3$ and $FAPbI_3$ NCs matching with that the cubic perovskite crystal structure; d) absorption and PL of $CsPbI_3$ and $FAPbI_3$ NCs. XRD reference pattern of $CsPbI_3$ corresponds to 98-018-1288.

To explore the versatility of the OLAM-I precursor, both inorganic ($CsPbI_3$) and hybrid organic-inorganic ($FAPbI_3$) perovskite NCs were synthesized, as reported in Figure 2 (see the SI for details on the synthesis). The bright red-emitting $CsPbI_3$ NCs were about 12 nm in size, with PL peak centered at 688 nm (1.80 eV) and full-width at half maximum (FWHM) of 33 nm (~86 meV). The bright near infrared-emitting $FAPbI_3$ NCs, about 14 nm in size, had a PL spectrum centered at 762 nm (1.62 eV) with FWHM of 64 nm (~138 meV). The freshly made solutions of $CsPbI_3$ and $FAPbI_3$ NCs had high PL quantum yields (PLQY) of 79±4% ($CsPbI_3$ NCs, under 510 nm excitation) and 74±3% ($FAPbI_3$ NCs, under 600 nm excitation). Both the $CsPbI_3$ and $FAPbI_3$ NCs evidenced multiexponential PL decays with similar 1/e lifetimes of ~40 ns under 508 nm pulsed excitation (Figure SI3). These red-emitting lead iodide perovskite NCs prepared from off-the-shelf chemicals under air on a hotplate had therefore optical properties on par with the ones synthesized under inert atmosphere with degassed precursors.[23] In addition to the emissive iodide perovskite NCs, wide-gap zero-dimensional Cs_4PbI_6 NCs could also be synthesized, simply by increasing the Cs:Pb ratio, as shown in Figure SI4.[10, 24]

We have exploited the excellent optical properties of the iodide perovskite NCs prepared with our simple approach to fabricate deep-red and infrared light-emitting diodes (LEDs). To remove excess ligands and ODE from the solution, a problem often limiting the use of NCs in devices,[25] a simple "rinsing" procedure was used (see experimental details in SI and scheme SI2). Here, after the NCs were separated from the growth solution through centrifugation, the vial was slowly (without shaking) filled with toluene, allowing for any residual organics attached to the vial to dissolve. The toluene was then removed, and the NCs were fully redispersed in toluene. The NCs samples to be used for LED fabrication were stored at high concentrations (6 times higher compared to normal storage). Under these conditions the NC were stable, as no significant loss of PL was seen after the samples were exposed to air for 2 weeks. The NC LEDs were prepared by spin-coating poly(3,4-ethylenedioxythiophene)-poly(styrenesulfonate) (PEDOT:PSS) on pre-patterned ITO/Glass coated glass substrates, followed by a layer of spin-coated NCs. The devices were finalized by evaporation of 2,4,6-Tris[3-(diphenylphosphinyl) phenyl]-1,3,5-triazine (PO-T2T) as hole blocking layer and Ca/Ag bi-layer metal contact (see SI for more details on device fabrication and Figure 3a for a schematic representation of the device stack and approximate energy levels). To prepare the mixed (Cs:FA)PbI_3 NC LEDs, which are reported among the highest EQE among red/NIR NC LEDs,[26] the $CsPbI_3$ and $FAPbI_3$ NCs solutions were simply mixed prior to devices fabrication. Due to interparticle cation exchange, the mixed solution exhibited a single PL peak and absorption centered between 688 nm and 762 nm, indicating a homogeneous (Cs:FA)PbI_3 composition.[17,23]

The electroluminescence spectra for all three devices (Figure 3b) evidenced single-peak emission at 688 nm ($CsPbI_3$), 728 nm (mixed Cs/$FAPbI_3$), and 739 nm ($FAPbI_3$). This corresponds to a deep-red emission for the inorganic NCs with CIE coordinates (0.6489, 0.2856), thus promising for wide-gamut displays and lighting and near-infrared emission for the $FAPbI_3$ and mixed-cation FA/$CsPbI_3$ NCs. Figure 3c reports the current-voltage-radiant flux curves of the three devices. The highest radiant flux was obtained for purely inorganic $CsPbI_3$ NCs, exceeding 10^6 μW/m^2 at 8 V. This corresponds to XXX cd/m^2 (compare the value in cd/m^2 with literature). However, the most efficient devices were obtained with mixed Cs/$FAPbI_3$, with external quantum efficiency (EQE) exceeding 2% in the whole range from 2,5 V to 7 V and an a maximum EQE over 3% around 4,3 V. These results are on par with record EQEs recently reported with NCs of similar chemical composition.[23,26] Contrary to the other two devices, the one based on pure $FAPbI_3$ evidenced a strong degradation of the radiance above 4V (Figure 3c) which ultimately led to lower EQE (Figure 3d). Interestingly, the incorporation of the inorganic cation Cs^+ in the mixed NCs resulted in an increase of over one order of magnitude in EQE (Figure 3d) while maintaining an emission maximum close to that of pure $FAPbI_3$ (Figure 3b).

The present synthesis approach could be easily extended to other iodide-based NCs in addition to the lead halide perovskites discussed above. As shown in Figures 4 and SI5, the injection of the iodine precursor in a ODE solution containing an alkali metal-oleate lead to the nucleation and growth of alkali iodide NCs with a narrow size distribution. The KI and RbI NCs crystallized in a simple cubic (Pm3m) crystal structure with cubic habit, whereas the CsI NCs crystalized into in a face centered cubic (Fm3m) crystal structure, with cubo-octahedral habit. Similar to reports of CsI NCs, all the alkali metal NCs had an absorption band at around 220-230 nm, as shown Figure SI6.[11] It is interesting to note the absorption band of these NCs is similar that of oleylammonium iodide (Figure SI7). These types of NCs should be interesting for use in scintillators, a common application for bulk CsI.

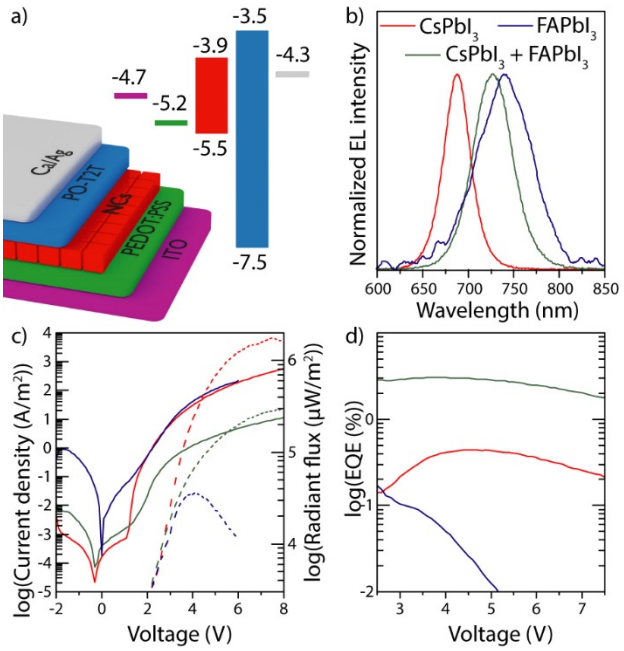

Figure 3. Device characteristics. (a) Schematic representation and flat band energy diagram of the LEDs used in this work (energy levels of the emitting material layer in the scheme correspond to $FAPbI_3$). (b) Normalized electroluminescent spectra, where red, blue and green curves refer to $CsPbI_3$, $FAPbI_3$ and mixed Cs/$FAPbI_3$, respectively. (c) Current-voltage-luminance and (d) EQE vs voltage characteristics of the NCs LEDs.

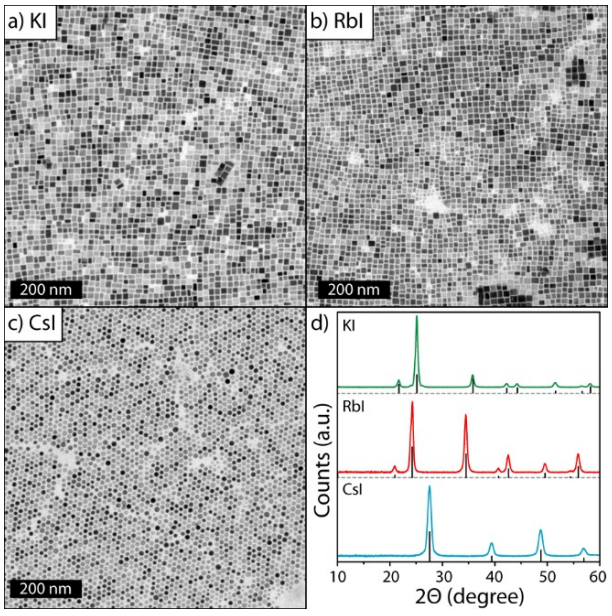

Figure 4. KI, RbI and CsI NCs. TEM image of monodisperse (a) 14 nm KI, (b) 16 nm RbI and (c) 14 nm CsI NC; d) XRD patterns of KI, RbI and CsI NCs matching with their respective reference patterns. XRD

reference patterns of KI, Rb and CsI correspond to 96-900-8655, 96-900-8711 and 96-900-8791 respectively.

The ability to introduce iodine independent from the metal precursors in the reaction flask allowed us to extend the OLAM-I method to the synthesis of lead-free ternary bismuth iodide NCs. As shown in Figure 5a-b, both $Cs_3Bi_2I_9$ and $FA_3Bi_2I_9$ NCs could be synthesized. Whereas $Cs_3Bi_2I_9$ and $MA_3Bi_2I_9$ have been extensively investigated, mainly with the aim to replace lead based perovskites in photovoltaic devices,[27-29] its organic formamidinium counterpart, $FA_3Bi_2I_9$, was only very recently reported as a bulk material.[30] Both $Cs_3Bi_2I_9$ and $FA_3Bi_2I_9$ NCs crystallized in the Cs_3CrCl_9 crystal structure (Figure 5c),[31] where isolated $[Bi_2I_9]^{3-}$ clusters made of two face-sharing octahedra are surrounded by ether Cs^+ or FA cations. Here, $FA_3Bi_2I_9$ is characterized by a slightly larger unit cell than $Cs_3Bi_2I_9$, due to the increased ionic radius of FA compared to that of Cs^+.[30] Similar to previous reports, the $Cs_3Bi_2I_9$ and $FA_3Bi_2I_9$ NCs had a strong excitonic abortion peak around 500 nm (Figure 5d), originating from the absorption of the single $[Bi_2I_9]^{3-}$ clusters, which is almost identical for $Cs_3Bi_2I_9$ and $FA_3Bi_2I_9$, as the monovalent cation has very little influence on the optical transitions within the $[Bi_2I_9]^{3-}$ clusters.

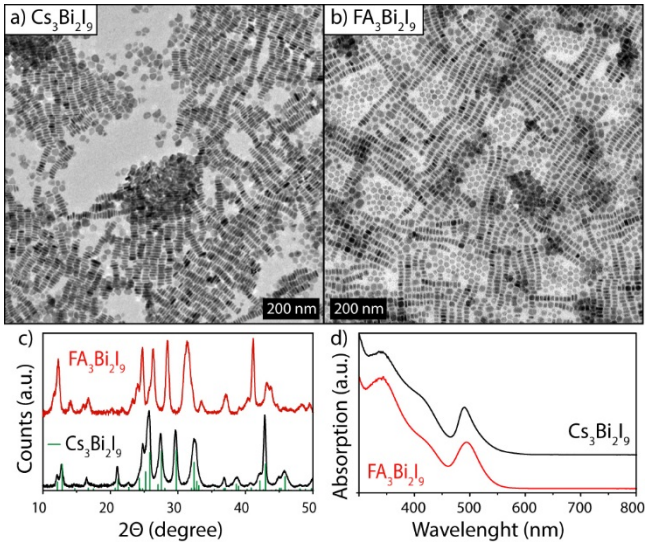

Figure 5. $Cs_3Bi_2I_9$ and $FA_3Bi_2I_9$ NCs. TEM images of monodisperse $Cs_3Bi_2I_9$ and $FA_3Bi_2I_9$ platelet shaped NCs, with their respective (c) XRD patterns and (d) absorption spectra. The XRD reference pattern of $Cs_3Bi_2I_9$ corresponds to 98-000-1448.

Finally, the OLAM-I approach was extended to the synthesis of binary and ternary silver iodide based NCs. As shown in Figure SI8, AgI NCs with a size of about 25 nm, and $RbAg_4I_5$ NCs of about 19 nm could be synthesized. $RbAg_4I_5$ is a superionic conductor which is characterized by a very high Ag^+ conductivity, even at low temperatures and is thus used as a solid electrolyte.[32-34] This makes $RbAg_4I_5$ a promising material for all-solid-state super capacitors.[35] The crystal structure of the $RbAg_4I_5$ NCs matches with that of previously reported $RbAg_4I_5$.[33]

Overall, we have presented a fast and tunable synthesis method for a wide variety of metal iodide NCs. This protocol gives access to high quality lead halide perovskite NCs with PLQYs above 70%, but can also be used to screen new metal iodide based NCs, like the here reported KI, RbI, $FA_3Bi_2I_9$ and $RbAg_4I_5$ NCs. The use of a simple hot plate, in air, based method with a room temperature and air stable iodide precursor should enable its exploitation in the high-throughput synthesis of NCs, using for instance synthesis robots, or droplet-based microfluidic reactors.[36-37] The high external quantum yield and narrow emission spectra obtained from LEDs incorporating the perovskite NCs confirms their high optical and electronic quality. Additionally, we demonstrate that the use of mixed NCs significantly improves the LED performance.

ASSOCIATED CONTENT

The Supporting Information is available free of charge on the ACS Publications website at DOI: xxxxx.

Experimental details of optical absorption, PL spectra, PLQY, PL lifetime measurements, PL decay curves

AUTHOR INFORMATION

Corresponding Author

*F. Palazon. E-mail: Francisco.Palazon@uv.es

*L. Manna. E-mail: liberato.manna@iit.it

ACKNOWLEDGMENT

The research leading to these results has received funding from the European Union seventh Framework Programme under Grant Agreement No. 614897 (ERC Consolidator Grant "TRANS-NANO") and framework Programme for Research and Innovation Horizon 2020 (2014-2020) under the Marie Skłodowska-Curie Grant Agreement PerovSAMs No. 747599. We also acknowledge financial support from the Spanish Ministry of Science, Innovation and Universities via the Unidad de Excelencia María de Maeztu MDM-2015-0538, MAT2017-88821-R.

REFERENCES

1. Protesescu, L.; Yakunin, S.; Bodnarchuk, M. I.; Krieg, F.; Caputo, R.; Hendon, C. H.; Yang, R. X.; Walsh, A.; Kovalenko, M. V. Nanocrystals of Cesium Lead Halide Perovskites ($CsPbX_3$, X = Cl, Br, and I): Novel Optoelectronic Materials Showing Bright Emission with Wide Color Gamut. *Nano Lett.* **2015,** *15*, 3692-3696.

2. Akkerman, Q. A.; Rainò, G.; Kovalenko, M. V.; Manna, L. Genesis, Challenges and Opportunities for Colloidal Lead Halide Perovskite Nanocrystals. *Nat. Mater.* **2018,** *17*, 394-405.

3. Kovalenko, M. V.; Protesescu, L.; Bodnarchuk, M. I. Properties and Potential Optoelectronic Applications of Lead Halide Perovskite Nanocrystals. *Science* **2017,** *358*, 745-750.

4. Schmidt, L. C.; Pertegás, A.; González-Carrero, S.; Malinkiewicz, O.; Agouram, S.; Mínguez Espallargas, G.; Bolink, H. J.; Galian, R. E.; Pérez-Prieto, J. Nontemplate Synthesis of $CH_3NH_3PbBr_3$ Perovskite Nanoparticles. *J. Am. Chem. Soc.* **2014,** *136*, 850-853.

5. Wang, A.; Yan, X.; Zhang, M.; Sun, S.; Yang, M.; Shen, W.; Pan, X.; Wang, P.; Deng, Z. Controlled Synthesis of Lead-Free and Stable Perovskite Derivative Cs_2SnI_6 Nanocrystals Via a Facile Hot-Injection Process. *Chem. Mater.* **2016,** *28*, 8132-8140.

6. Qiu, X., et al. From Unstable Cssni$_3$ to Air-Stable Cs_2SnI_6: A Lead-Free Perovskite Solar Cell Light Absorber with Bandgap of 1.48 Ev and High Absorption Coefficient. *Sol. Energy Mater. Sol. Cells* **2017,** *159*, 227-234.

7. Zhang, J.; Yang, Y.; Deng, H.; Farooq, U.; Yang, X.; Khan, J.; Tang, J.; Song, H. High Quantum Yield Blue Emission from Lead-Free Inorganic Antimony Halide Perovskite Colloidal Quantum Dots. *ACS Nano* **2017,** *11*, 9294-9302.

8. Zhang, Y.; Yin, J.; Parida, M. R.; Ahmed, G. H.; Pan, J.; Bakr, O. M.; Brédas, J.-L.; Mohammed, O. F. Direct-Indirect Nature of the Bandgap in Lead-Free Perovskite Nanocrystals. *J. Phys. Chem. Lett.* **2017,** *8*, 3173-3177.

9. Sun, J.; Yang, J.; Lee, J. I.; Cho, J. H.; Kang, M. S. Lead-Free Perovskite Nanocrystals for Light-Emitting Devices. *J. Phys. Chem. Lett.* **2018,** *9*, 1573-1583.

10. Akkerman, Q. A., et al. Nearly Monodisperse Insulator Cs_4PbX_6 (X = Cl, Br, I) Nanocrystals, Their Mixed Halide Compositions, and Their Transformation into $CsPbX_3$ Nanocrystals. *Nano Lett.* **2017,** *17*, 1924-1930.

11. Shamsi, J.; Dang, Z.; Ijaz, P.; Abdelhady, A. L.; Bertoni, G.; Moreels, I.; Manna, L. Colloidal CsX (X = Cl, Br, I) Nanocrystals and Their Transformation to $CsPbX_3$ Nanocrystals by Cation Exchange. *Chem. Mater.* **2017,** *30*, 79-83.

12. Akkerman, Q. A.; Meggiolaro, D.; Dang, Z.; De Angelis, F.; Manna, L. Fluorescent Alloy $CsPb_xMn_{1-x}I_3$ Perovskite Nanocrystals with High Structural and Optical Stability. *ACS Energy Lett.* **2017,** *2*, 2183-2186.

13. Liu, H.; Owen, J. S.; Alivisatos, A. P. Mechanistic Study of Precursor Evolution in Colloidal Group II–Vi Semiconductor Nanocrystal Synthesis. *J. Am. Chem. Soc.* **2007,** *129*, 305-312.

14. Hendricks, M. P.; Campos, M. P.; Cleveland, G. T.; Jen-La Plante, I.; Owen, J. S. A Tunable Library of Substituted Thiourea Precursors to Metal Sulfide Nanocrystals. *Science* **2015,** *348*, 1226-1230.

15. Creutz, S. E.; Crites, E. N.; De Siena, M. C.; Gamelin, D. R. Colloidal Nanocrystals of Lead-Free Double-Perovskite (Elpasolite) Semiconductors: Synthesis and Anion Exchange to Access New Materials. *Nano Lett.* **2018,** *18*, 1118-1123.

16. Imran, M.; Caligiuri, V.; Wang, M.; Goldoni, L.; Prato, M.; Krahne, R.; De Trizio, L.; Manna, L. Benzoyl Halides as Alternative Precursors for the Colloidal Synthesis of Lead-Based Halide Perovskite Nanocrystals. *J Am Chem Soc* **2018,** *140*, 2656-2664.

17. Akkerman, Q. A.; D'Innocenzo, V.; Accornero, S.; Scarpellini, A.; Petrozza, A.; Prato, M.; Manna, L. Tuning the Optical Properties of Cesium Lead Halide Perovskite Nanocrystals by Anion Exchange Reactions. *J. Am. Chem. Soc.* **2015,** *137*, 10276-10281.

18. Schug, J. C.; Kogan, M. J. The Nature of Iodine-Amine Solutions. *J. Magn. Reson.* **1973,** *11*, 406-415.

19. Gardner, J. M.; Abrahamsson, M.; Farnum, B. H.; Meyer, G. J. Visible Light Generation of Iodine Atoms and I–I Bonds: Sensitized I^- Oxidation and I^{3-} Photodissociation. *J. Am. Chem. Soc.* **2009,** *131*, 16206-16214.

20. Im, J.-H.; Lee, C.-R.; Lee, J.-W.; Park, S.-W.; Park, N.-G. 6.5% Efficient Perovskite Quantum-Dot-Sensitized Solar Cell. *Nanoscale* **2011,** *3*, 4088-4093.

21. Wan, L.; Xu, Y. Iodine-Sensitized Oxidation of Ferrous Ions under Uv and Visible Light: The Influencing Factors and Reaction Mechanism. *Photochem. Photobiol. Sci.* **2013,** *12*, 2084-2088.

22. Almeida, G.; Goldoni, L.; Akkerman, Q.; Dang, Z.; Khan, A. H.; Marras, S.; Moreels, I.; Manna, L. Role of Acid-Base Equilibria in the Size, Shape, and Phase Control of Cesium Lead Bromide Nanocrystals. *ACS Nano* **2018,** *12*, 1704-1711.

23. Protesescu, L., et al. Dismantling the "Red Wall" of Colloidal Perovskites: Highly Luminescent Formamidinium and Formamidinium–Cesium Lead Iodide Nanocrystals. *ACS Nano* **2017,** *11*, 3119-3134.

24. Akkerman, Q. A.; Abdelhady, A. L.; Manna, L. Zero-Dimensional Cesium Lead Halides: History, Properties, and Challenges. *J. Phys. Chem. Lett.* **2018,** *9*, 2326-2337.

25. Boles, M. A.; Ling, D.; Hyeon, T.; Talapin, D. V. The Surface Science of Nanocrystals. *Nat. Mater.* **2016,** *15*, 141-153.

26. Lignos, I., et al. Exploration of near-Infrared-Emissive Colloidal Multinary Lead Halide Perovskite Nanocrystals Using an Automated Microfluidic Platform. *ACS Nano* **2018,** *12*, 5504-5517.

27. Ghosh, B.; Wu, B.; Mulmudi, H. K.; Guet, C.; Weber, K.; Sum, T. C.; Mhaisalkar, S. G.; Mathews, N. Limitations of $Cs_3Bi_2I_9$ as Lead-Free Photovoltaic Absorber Materials. *ACS Appl. Mater. Interfaces.* **2018**.

28. Yang, B., et al. Lead-Free, Air-Stable All-Inorganic Cesium Bismuth Halide Perovskite Nanocrystals. *Angew. Chem.* **2017,** *129*, 12645-12649.

29. Zhang, Z.; Li, X.; Xia, X.; Wang, Z.; Huang, Z.; Lei, B.; Gao, Y. High-Quality $(CH_3NH_3)_3Bi_2I_9$ Film-Based Solar Cells: Pushing Efficiency up to 1.64%. *J. Phys. Chem. Lett.* **2017,** *8*, 4300-4307.

30. Shin, S. S.; Correa Baena, J. P.; Kurchin, R. C.; Polizzotti, A.; Yoo, J. J.; Wieghold, S.; Bawendi, M. G.; Buonassisi, T. Solvent-Engineering Method to Deposit Compact Bismuth-Based Thin Films: Mechanism and Application to Photovoltaics. *Chem. Mater.* **2018,** *30*, 336-343.

31. J., W. G.; W., I. D. J. The Crystal Structure of $Cs_3Cr_2Cl_9$. *Acta Crystallogr.* **1957,** *10*, 466-468.

32. Owens, B. B.; Argue, G. R. High-Conductivity Solid Electrolytes: MAg_4I_5. *Science* **1967,** *157*, 308-310.

33. Geller, S. Crystal Structure of the Solid Electrolyte, $RbAg_4I_5$. *Science* **1967,** *157*, 310-312.

34. Hull, S.; Keen, D. A.; Sivia, D. S.; Berastegui, P. Crystal Structures and Ionic Conductivities of Ternary Derivatives of the Silver and Copper Monohalides: I. Superionic Phases of Stoichiometry MA_4I_5:$RbAg_4I_5$, KAg_4I_5, and KCu_4I_5. *J. Solid State Chem.* **2002,** *165*, 363-371.

35. Chen, C.-C.; Fu, L.; Maier, J. Synergistic, Ultrafast Mass Storage and Removal in Artificial Mixed Conductors. *Nature* **2016,** *536*, 159–164.

36. Chan, E. M.; Xu, C.; Mao, A. W.; Han, G.; Owen, J. S.; Cohen, B. E.; Milliron, D. J. Reproducible, High-Throughput Synthesis of Colloidal Nanocrystals for Optimization in Multidimensional Parameter Space. *Nano Lett.* **2010,** *10*, 1874-1885.

37. Lignos, I.; Stavrakis, S.; Nedelcu, G.; Protesescu, L.; deMello, A. J.; Kovalenko, M. V. Synthesis of Cesium Lead Halide Perovskite Nanocrystals in a Droplet-Based Microfluidic Platform: Fast Parametric Space Mapping. *Nano Lett.* **2016,** *16*, 1869-1877.

Insert Table of Contents artwork here